Available online at www.sciencedirect.com

ScienceDirect

Advances in Space Research xxx (2013) xxx–xxx

ADVANCES IN SPACE RESEARCH (a COSPAR publication)

www.elsevier.com/locate/asr

Effects on winter circulation of short and long term solar wind changes

Limin Zhou [a], Brian Tinsley [b,*], Jing Huang [a]

[a] Key Laboratory of Geographic Information Science, East China Normal University, China
[b] University of Texas at Dallas, Richardson, TX 75080, USA

Abstract

Indices of the North Atlantic Oscillation and the Arctic Oscillation show correlations on the day-to-day timescale with the solar wind speed (SWS). Minima in the indices were found on days of SWS minima during years of high stratospheric aerosol loading. The spatial distribution of surface pressure changes during 1963–2011 with day-to-day changes in SWS shows a pattern resembling the NAO. Such a pattern was noted for year-to-year variations by Boberg and Lundstedt (2002), who compared NAO variations with the geo-effective solar wind electric field (the monthly average SWS multiplied by the average southward component, i.e., negative Bz component, of the interplanetary magnetic field). The spatial distribution of the correlations of geopotential height changes in the troposphere and stratosphere with the SWS; the geo-effective electric field (SWS*Bz); and the solar 10.7 cm flux suggests that solar wind inputs connected to the troposphere via the global electric circuit, together with solar ultraviolet irradiance acting on the stratosphere, affect regional atmospheric dynamics.

Keywords: Arctic Oscillation; North Atlantic Oscillation; Solar wind speed; Relativistic electrons; Global electric circuit

1. Introduction

There is much uncertainty about the mechanism(s) of observed linkages between solar activity and weather and climate change, while there is a wealth of data to show that such linkages exist (a few examples are as in Roberts and Olson, 1973; Eddy, 1976; Fleitmann et al., 2003; Wang et al., 2005). Responses of the lower atmosphere to space weather for short timescales (a few hours to a few days) as well as long timescales (seasonal to decadal) have been observed. Changes in tropospheric dynamics are found to correlate on short time scales with solar wind parameters such as its speed and the components of its magnetic field. In addition, longer term tropospheric and stratospheric changes correlate with total solar irradiance and solar ultraviolet irradiance as well as space weather parameters (Gray et al., 2010). The influences of energetic space particles and space electric and magnetic fields can potentially account for some of the variability in the lower atmosphere, such as in cloud cover (Marsh and Svensmark, 2003; Kniveton and Tinsley, 2004) polar surface pressure (Burns et al., 2008) and winter cyclone vorticity (Roberts and Olson, 1973; Svalgaard, 1973; Tinsley and Deen, 1991; Veretenenko and Thejll, 2004; Tinsley et al., 2012).

A correlation between the interplanetary magnetic field (IMF) direction changes and changes in the vorticity of winter storms (represented by the Vorticity Area Index or VAI) was found by Wilcox et al. (1973) and confirmed by the later work by Kirkland et al. (1996) and Tinsley et al. (1994, 2012). The changes in the IMF direction occur as the heliospheric current sheets, that form the boundaries of solar wind magnetic sectors, pass over the Earth (HCS crossings), and the later work showed that these also coincide with changes in the solar wind speed (SWS) and the precipitation of relativistic electrons from the radiation belts. The VAI was defined by Roberts and Olson (1973), for extended winters, November through March, for latitudes poleward of 20°N, and for 300 hPa levels in the

* Corresponding author. Tel.: +1 9728832838.
E-mail addresses: lmzhou@geo.ecnu.edu.cn (L. Zhou), tinsley@utdallas.edu (B. Tinsley).

0273-1177/$36.00 © 2013 COSPAR. Published by Elsevier Ltd. All rights reserved.
http://dx.doi.org/10.1016/j.asr.2013.09.017

atmosphere, but can be evaluated for any latitude range; for any pressure level; with any threshold vorticity, and for any months. Systematic changes in the strength of cyclogenesis, measured by the VAI in a given hemisphere, affect the amplitude of Rossby waves, and these changes in atmospheric circulation, downstream of a cyclogenesis center, can affect regional climate. The short time scale of the day-to-day VAI responses avoids the confounding effects, such as cycles from ocean–atmosphere coupling, present in longer term atmospheric variability.

Starting from monthly averages, Boberg and Lundstedt (2002, 2003) constructed a proxy (E) for the solar wind geo-effective electric field, by taking the monthly average SWS and multiplying it by the monthly mean of the negative IMF Bz component. With negative Bz there is stronger coupling of solar wind energy into the magnetosphere for a given SWS than for positive Bz. They found that there was strong correlation between annual mean value of E and atmospheric pressure and temperature distributions that resembled the North Atlantic Oscillation (NAO). The NAO index (Visbeck et al., 2001) is the sea-level pressure difference between stations in the northern Atlantic (e.g. Iceland) and subtropical Atlantic (e.g., the Azores). Boberg and Lundstedt (2002, 2003) showed strong responses in both the high altitude region (above the 50 hPa level) as well as in the troposphere, and concluded that the high altitude change due to the solar wind geo-effective electric field subsequently propagated down into the troposphere. Downward propagation of zonal wind perturbations from the stratosphere can result in changes in the tropospheric circulation patterns. Baldwin and Dunkerton (2001) and Reichler et al. (2012) showed that changes in the stratospheric mean flow could influence the development of circulation patterns such as the NAO, with the downward propagation taking between 15 and 50 days. Because of this propagation time, such downward propagation cannot be the cause of the tropospheric responses to the solar wind input with a time delay no more than a day. Furthermore, stratospheric mean flow anomalies that propagate downward to induce tropospheric circulation patterns, such as the NAO, may not necessarily be due to external forcing of the stratosphere (e.g., by particle precipitation affecting ozone chemistry, or by solar UV changes). Baldwin and Dunkerton (2001) and Reichler et al. (2012) noted that the modification of the stratospheric mean flow that influences tropospheric circulation could be due to waves originating in the troposphere. Reichler et al. (2012) used a model with no external forcing to generate strong stratospheric zonal flow anomalies that then propagated down to the troposphere. They suggested that stochastic forcing from the troposphere, producing dynamic wave forcing of the stratospheric flow, was responsible for the stratospheric zonal flow anomalies. Thus a direct forcing of the troposphere from the solar wind, as suggested by Tinsley (2012) due to invigoration of cyclones due to changes in cloud microphysics, that respond to the current flow in the global electric circuit forced by the solar wind, could be a source of dynamic waves affecting stratospheric flow. On the other hand, there is evidence for changes in the mean flow and temperature of the stratosphere caused by UV and QBO and energetic particle forcing (Gray et al., 2010), so several mechanisms could be contributing to the observed stratospheric responses to solar activity.

The responses on the day to day time scale have been shown to involve both the relativistic electron flux (REF), precipitating from the radiation belts at subauroral latitudes, and stratospheric volcanic aerosols. A strong correlation between the REF and the SWS has been examined by Li et al (2001a,b). Tinsley et al. (1994, 2012) described a link between space weather and lower atmospheric dynamics through the global electric circuit. Minima in the SWS and deep minima in the REF are associated with the HCS crossings, as shown by Tinsley et al. (1994, Fig. 5). The REF can penetrate down to upper stratospheric levels, and the Bremsstrahlung radiation that they produce can impact the electric conductivity down to lower stratospheric levels and change the stratospheric electrical column resistance. The consequent changes in the ionosphere-earth current density (Jz) that flows as the downward return current in the global electric circuit was considered to be the physical link to the tropospheric cloud and dynamical changes, especially when there is high stratosphere aerosol loading due to volcanic eruptions, which will increase the proportion of the stratospheric column resistance to that of the whole atmosphere column. Observations of minima in tropospheric potential gradient and Jz at HCS crossings have been reported by Reiter (1977), and Fischer and Mühleisen (1980) also observed such potential gradient minima.

According to the hypothesis of Tinsley et al. (1994) this effect is considered to occur for several years following volcanic eruptions that inject large quantities of SO_2 gas into the stratosphere. This SO_2 forms H_2SO_4 on a timescale of months, followed by production of ultrafine aerosol particles from the gaseous H_2SO_4 (Goodman et al., 1994). When carried into the higher temperatures of the upper stratosphere by the Brewer–Dobson circulation, the aerosol particles formed in the lower stratosphere evaporate and/or are dissociated by radiation and become gaseous, but re-condense to form ultrafine aerosol particles as the air descends and diabatically cools in the downward branches of the circulation. Fig. 1 illustrates the variations in stratospheric aerosol content from 1850 to the present.

In this work the responses of Northern Hemispheric Annual Mode (AO index), NAO index, and surface pressure to SWS changes on the day-to-day timescale during the period 1963–2011 are evaluated. The AO index (Thompson and Wallace, 1998) is the leading empirical orthogonal pattern of sea level pressure anomalies. Both the AO and the NAO are indicators of baroclinicity, or the intensity of the general circulation in the North Atlantic, with the AO representing a larger area than the NAO. In winter the baroclinicity is one of the drivers for cyclogenesis in the north Atlantic. With positive NAO or AO

Please cite this article in press as: Zhou, L., et al. Effects on winter circulation of short and long term solar wind changes. J. Adv. Space Res. (2013), http://dx.doi.org/10.1016/j.asr.2013.09.017

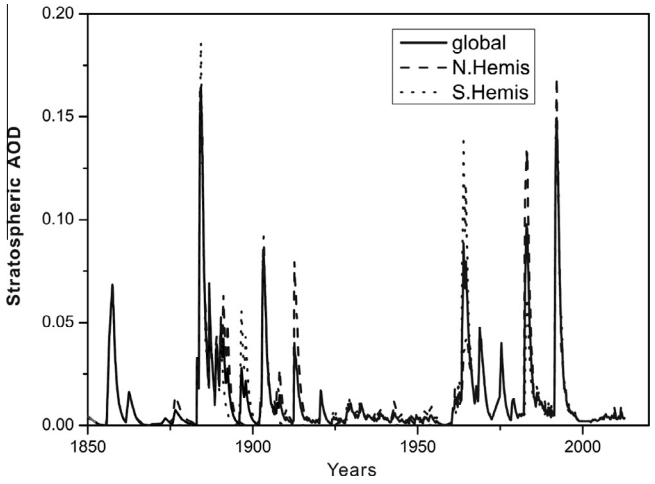

Fig. 1. The optical depth in the stratosphere. The solid line is the average for the whole globe; the dashed line is the average for the Northern Hemisphere; the dotted line is the average for the Southern hemisphere. (from NASA Goddard Institute for Space Studies).

phase there are more intense and more frequent storm moving from southwest to northeast across the Atlantic. With a negative NAO or AO phase the intensity and frequency of the storms is reduced. An investigation of data divided according to periods with higher and lower concentrations of stratospheric volcanic aerosols is made.

For long-term responses the correlations of SWS with surface pressure and geopotential height at five pressure levels of the Northern winter season (mean of December–January–February as DJF) and annual mean are investigated, together with similar correlations for E (the Boberg and Lundstedt proxy for the geo-effective solar wind electric field). A comparison is also made with correlations of the same atmospheric parameters with the F10.7 cm solar flux, as a proxy for the solar ultraviolet flux effects.

2. Data sources

The stratospheric aerosol optical depth data are from the NASA Goddard Institute for Space Studies web site, (http://data.giss.nasa.gov/modelforce/strataer/). The daily and monthly AO and NAO indices are obtained from the NOAA Climate Prediction Center (http://cpc.ncep.noaa.gov/products/precip/CWlink). Gridded monthly pressure at the surface and geopotential height data for five pressure levels (1000 hPa, 500 hPa, 100 hPa, 50 hPa, 10 hPa) are obtained from the NCAR–NCEP reanalysis data base (http://www.esrl.noaa.gov/psd/data/gridded/data.ncep.reanalysis.html). The IMF and SWS data are obtained from the OMNI time series (ftp://nssdcftp.gsfc.nasa.gov). The minima in the SWS were identified using the same criteria as in Mironova et al. (2012). The SWS data are intermittent from 1964 to 1994, but almost continuous thereafter. The relativistic electron flux is from LANL satellite measurements (Reeves et al., 2011, and auxiliary material), but supplemented by GOES measurements. The cosmic ray flux data are from the Moscow neutron monitor (http://www.ngdc.noaa.gov/stp/solar/cosmic.html). The 10.7 solar flux and sunspot number data are obtained from NOAA (http://www.ngdc.noaa.gov/nndc/struts). It should be noted that the high stratospheric volcanic aerosol eras tend to occur in years of low or declining sunspot number and 10.7 cm flux.

3. Results

3.1. Day to day response of the atmosphere parameters to SWS minima

Fig. 2 shows a set of superposed epoch analysis results for the response of NAO index (a) and (d), AO index (b) and (e), and SWS itself (c) and (g) with the key day being minima in the SWS in winters (November–March). Panels (a)–(c) are the results for 740 minima events in the low volcanic activity eras and the panels (d)–(g) are for the 147 minima events in high volcanic activity eras (1963–1966, 1983–1985 and 1993–1995) following the volcanic eruptions of the Mt. Agung, El Chicon and Pinatubo. These eruptions produced the last three prominent peaks of stratosphere aerosol seen in Fig. 1. In the low volcanic activity eras there is no clear response for all three indices, but in the high volcanic activity eras there is a clear response of all the indices to the SWS dip. The NAO index has an excursion of about 0.3 over the mean of 0.05 with 95% confidence by t-test; the AO index has an excursion of about 0.3 over the mean of −0.5, with 90% confidence by t-test. The minimum of NAO is at the same day of minima of SWS; the minimum of AO is one day after the key day.

Fig. 3 further separates the 147 high volcanic activity events according to whether Bz was negative or positive during the day of the SWS minimum, in order to test whether the geo-effectiveness of the solar wind coupling into the magnetosphere affected the day-to-day responses. There are differences between the responses to the geo-effective minima (Bz negative) in panels (a) through (c) and the remaining minima with Bz positive panels (d)–(f). For the NAO (a) and AO (b) there is a rise from about day −10 to day −3, and a sharp drop to a minimum on day 0. For the Bz positive conditions the NAO (d) and AO (e) also show dips of about the same amplitude on day 0, but there is less variability during the 30 days either side of day 0.

Fig. 4 shows a set of superposed epoch analysis results for the response to SWS minima of 10.7 cm solar flux (a) and (e), sunspot number (b) and (f) and galactic cosmic ray flux (c) and (g) with the same key day list for the same low and high volcanic activity eras as in Fig. 2. There is a slight increase (0.3%) in the cosmic ray flux (measured at Moscow), but this amplitude is an order of magnitude smaller than that which causes detectable responses (Tinsley and Deen, 1991). The results show that with the minima of SWS there is no significant relationship to sunspot number or to F10.7 (representing the solar UV emission).

Please cite this article in press as: Zhou, L., et al. Effects on winter circulation of short and long term solar wind changes. J. Adv. Space Res. (2013), http://dx.doi.org/10.1016/j.asr.2013.09.017

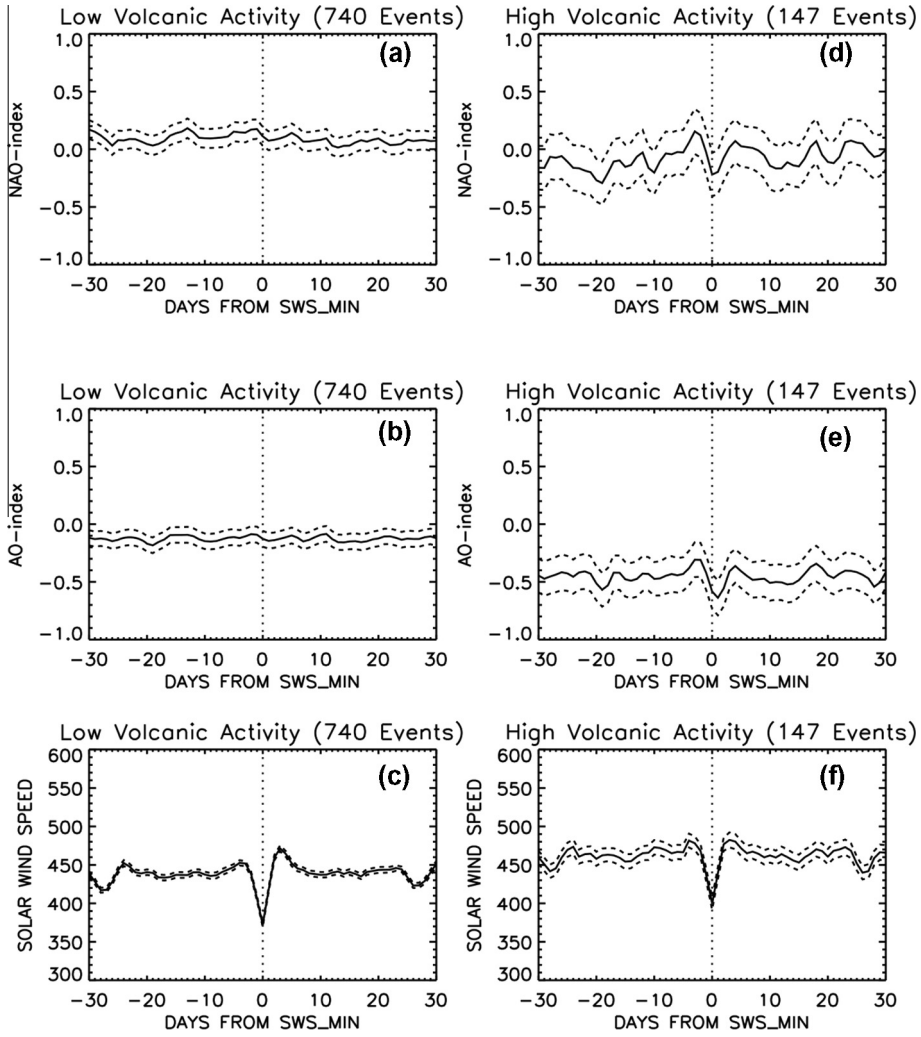

Fig. 2. Superposed epoch analyses of daily values of NAO (a) and (d), AO (b) and (e) and the SWS itself in km/s (c) and (f), with the key days being minima in the SWS in winters (November–March). The low-volcanic eras (1967–1983, 1985–1993 and 1995–2011) are on the left (a)–(c) and the high volcanic eras (November 1963–March 1966, November 1983–March 1985, November 1993–March 1995) are on the right (d)–(f). The solid lines are the mean of parameters of all the events and the dashed lines are the error of the mean value.

Fig. 5 shows the superposed epoch analysis results for the response to SWS minima of SWS itself (a) and (c) and relativistic electron flux (b) and (d) from 1989 to 2010. Continuous REF is available since 1989, and the relationship to SWS can be examined without considering volcanic aerosols, which do not affect geosynchronous altitudes. Panels (a) and (b) are for Bz positive on the key day, and panels (c) and (d) are for Bz negative. The minima in the REF in (b) and (d) occur one day after the minimum of the solar wind speed. For Bz positive on the key day there is a large increase during the recovery of the REF compared to the Bz negative condition. The asymmetry in Fig. 5 between relativistic electron fluxes before and after the SWS minima in (b) and (d), for Bz positive and negative on day 0, are consistent with the tendency for magnetic sector boundaries to occur on average one day after the SWS minima (Tinsley, 2005, Fig. 8). So Bz on day 0 tends to be the same as Bz in the sector preceding the SWS minimum, with the opposite Bz in the following sector. As noted earlier, negative Bz is associated with more geo-effective solar wind disturbances, including greater REF precipitation. This association is also relevant to the results of Fig. 3.

Fig. 6 shows a map of the response of the surface pressure to the minima to the solar wind speed in winter (DJF). The response is treated as the surface pressure difference between the day of the minimum, P_{min} and day −3 (the left shoulder), P_{sh}, i.e., as $P_{diff} = P_{min} - P_{sh}$. The results show that there are larger amplitude responses in the northern hemisphere than in the southern hemisphere, with the areas of significant responses about the same. The maximum significant positive response (with 99% confidence by *t*-test) lies in the eastern far north Atlantic Ocean with the center at 3°E, 65°N and a pressure enhancement over 4 hPa. The maximum significant negative response (with 99% confidence by *t*-test) appears in the West Atlantic Ocean region with the center at 54°W, 52°N and a pressure dip over 4 hPa.

Please cite this article in press as: Zhou, L., et al. Effects on winter circulation of short and long term solar wind changes. J. Adv. Space Res. (2013), http://dx.doi.org/10.1016/j.asr.2013.09.017

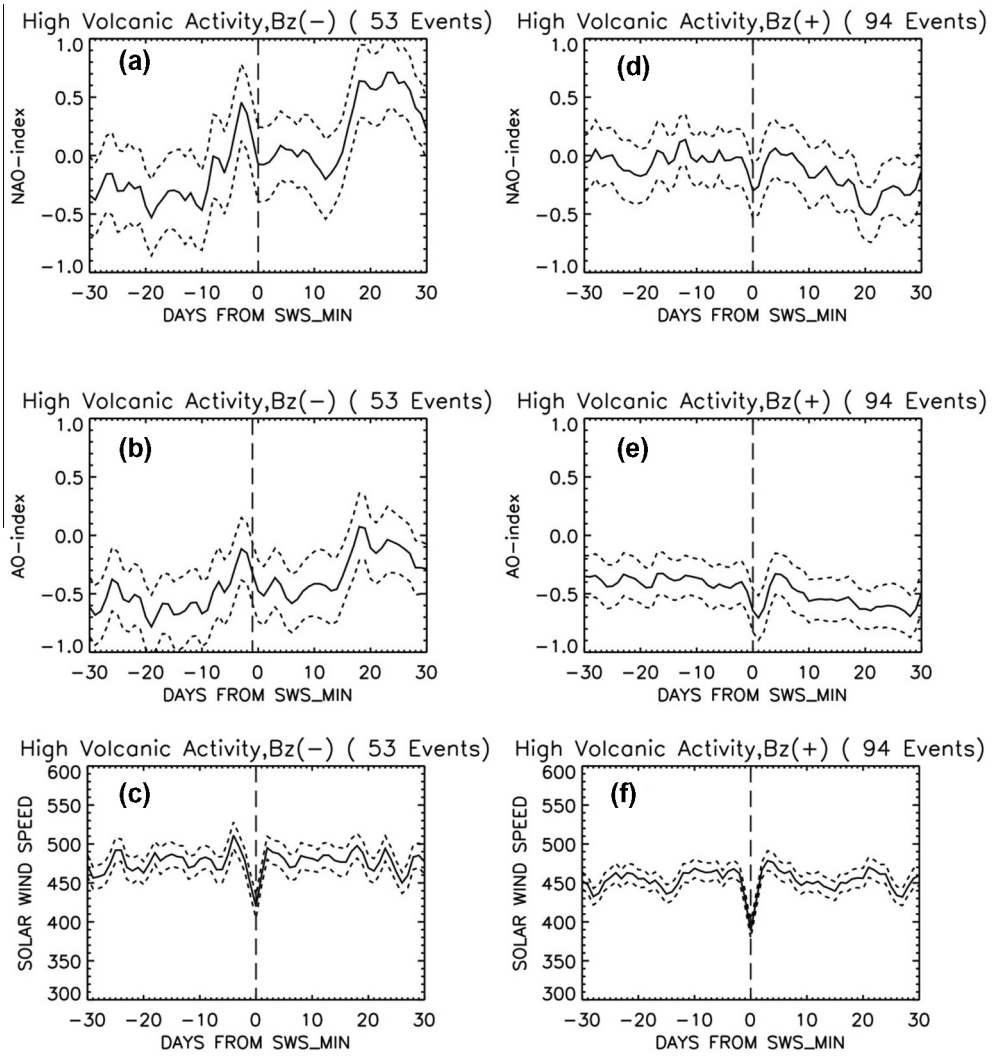

Fig. 3. As for Fig. 2, but with the 147 epochs for high volcanic activity separated into the 53 geo-effective SWS minima with Bz negative on day 0 (a)–(c) on the left, and the remaining 94 SWS minima with Bz positive on day 0 (d)–(f) on the right.

3.2. Long term correlation between atmosphere parameters and solar parameters

A longer term response of the climate indices to the SWS and to other solar activity parameters is explored by cross correlations. Table 1 shows the correlation between SWS, sunspot number, 10.7 cm solar flux, solar wind geo-effective electric field (E) as defined by Boberg and Lundstdt (2002), the NAO, and the AO, in the means for northern hemisphere winters (DJF), for the years 1963–2011. Table 1a is for the whole period of 1963–2011, Table 1b is for the high volcanic activity eras as in Fig. 2 and Table 1c is for the low volcanic activity eras as in Fig. 2. For all winters for 1963 to 2011 the SWS has significant correlations of 45.4% with 99% confidence with the NAO and 33.2% with 95% confidence for the AO. No significant correlations (even for 90% confidence) could be found for the NAO and AO with sunspot number, 10.7 cm solar flux and solar wind geo-effective electric field (E). As expected there are significant correlations on these monthly/annual timescales between E and sunspot number (71.6% with 99% confidence) and with 10.7 cm solar flux (65.8% with 99% confidence), and these are essentially the same for high and low volcanic activity.

For winters in high volcanic activity eras, (Table 1b) the correlations between SWS and NAO is increased, as also between the SWS and the AO, while the confidences are decreased (consistent with the smaller numbers of samples). However, the correlations of the NAO and AO with sunspot number, 10.7 cm flux, and SWS*Bz (i.e., with E) also increases, as do all the correlation of SWS*Bz with SWS, NAO and AO. The fact that much of time during each of the three eras of volcanic activity, the solar activity was declining and there were well developed high speed streams in the solar wind may be relevant to this result.

For winters in the low volcanic activity eras (Table 1c), the correlation results are slightly lower and less significant than those for the whole period in Table 1a, presumably as a result of the removal of the high volcanic winters with high correlations of Table 1b.

Please cite this article in press as: Zhou, L., et al. Effects on winter circulation of short and long term solar wind changes. J. Adv. Space Res. (2013), http://dx.doi.org/10.1016/j.asr.2013.09.017

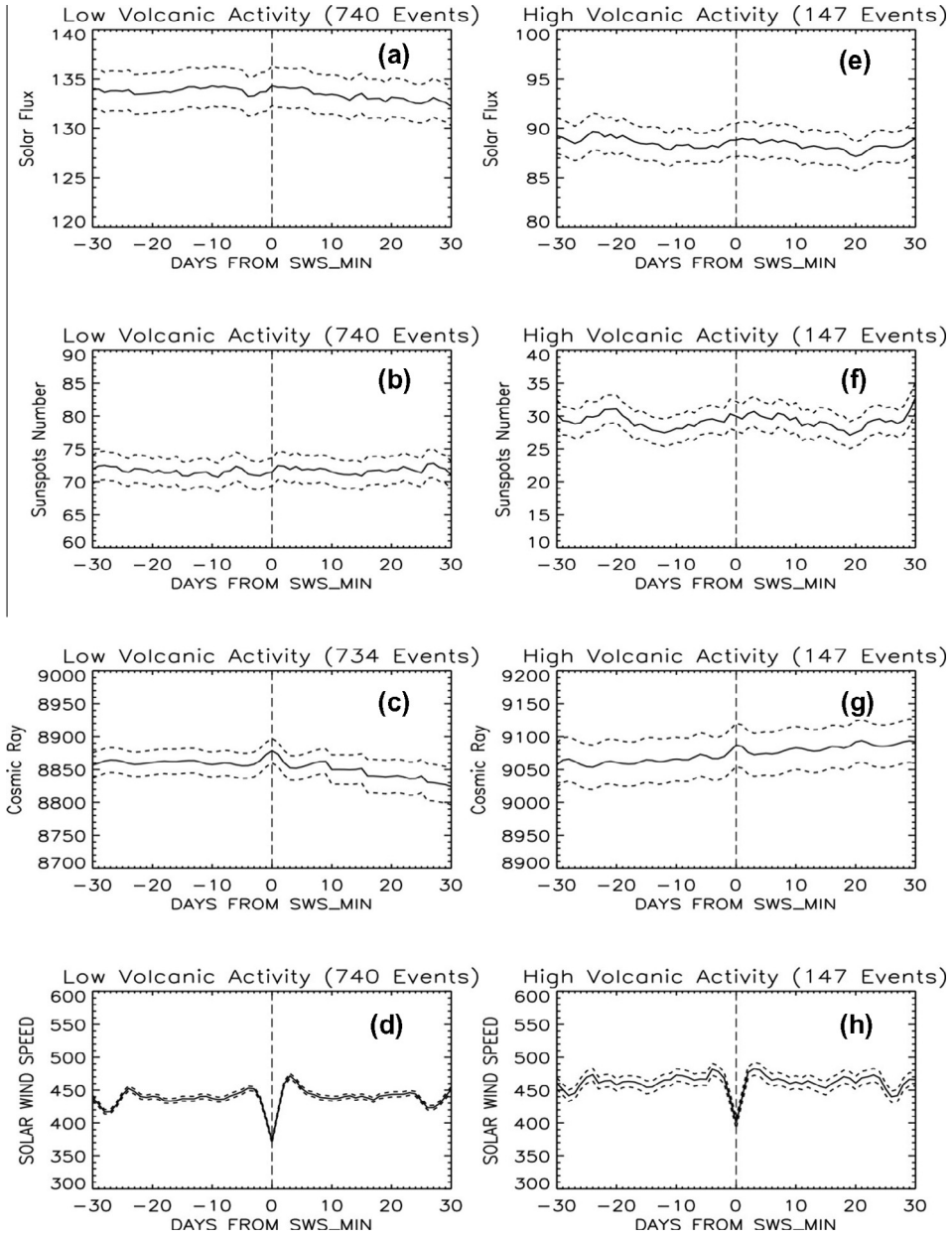

Fig. 4. As for Fig. 2, but for daily values of solar flux (10^{-22} W m^{-2} Hz^{-1}) (a) and (e), sun spot number (b) and (f), galactic cosmic ray flux (number/h) (c) and (g) and the SWS itself in km/s (d) and (h). The key days are minima in the SWS in winters (November–March) as before.

Figs. 7–9 show the spatial distribution of the correlation for winter averages (DJF) for five pressure levels (a)–(e) between geopotential height and the SWS (Fig. 7); or the 10.7 cm solar flux (Fig. 8); or solar wind geo-effective electric field (Fig. 9). In Fig. 7 at 1000 hPa a significant negative correlation (over 99% confidence) between SWS and geopotential height, with the center ranging from latitude 60°N to 70°N and longitude near 10°W–35°E, can be seen in the far northern Atlantic Ocean. There is also a significant positive correlation in the mid-latitude Atlantic Ocean at the latitude range from 10°N to 40°N. The positive and negative correlations weaken with height. At stratospheric levels (50 hPa and 10 hPa) the positive correlations cannot be seen, and the negative correlation has weakened and moved eastwards.

In Fig. 8 at 1000 hPa there is only a small region of eastern Europe that shows a significant negative correlation (over 99% confidence) between 10.7 cm solar flux and geopotential height, and there is no significant positive correlation. In the middle and high troposphere region, there is no clear correlation. With the increase of altitude, the stronger (over 70%) and significant (over 99% confidence) correlation appears in the stratosphere for the low latitude region equatorward of 30°N in the northern hemisphere and of 60°S in the southern hemisphere, and it is greater at higher stratospheric altitudes. During these northern winters it is

Please cite this article in press as: Zhou, L., et al. Effects on winter circulation of short and long term solar wind changes. J. Adv. Space Res. (2013), http://dx.doi.org/10.1016/j.asr.2013.09.017

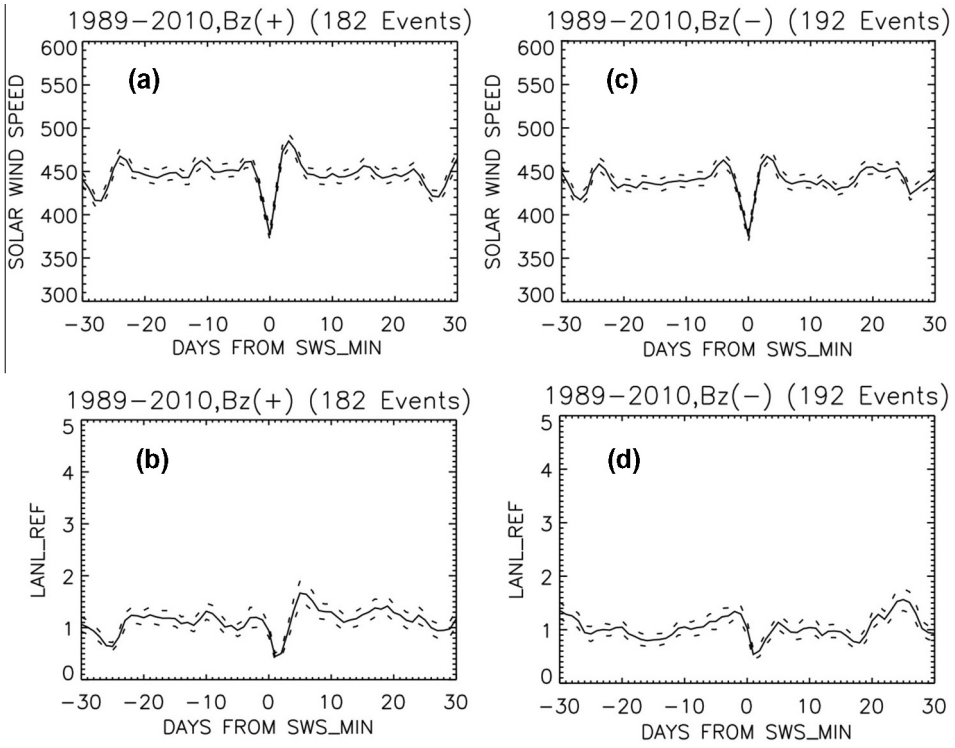

Fig. 5. Superposed epoch analyses of daily values of the SWS in km/s (a) and (c) and relativistic electron flux (b) and (d) with the key days being minima in the SWS in winters (November–March) from 1989 to 2010. Panels (a) and (b) are for positive Bz on the key day, while (c) and (d) are for negative Bz.

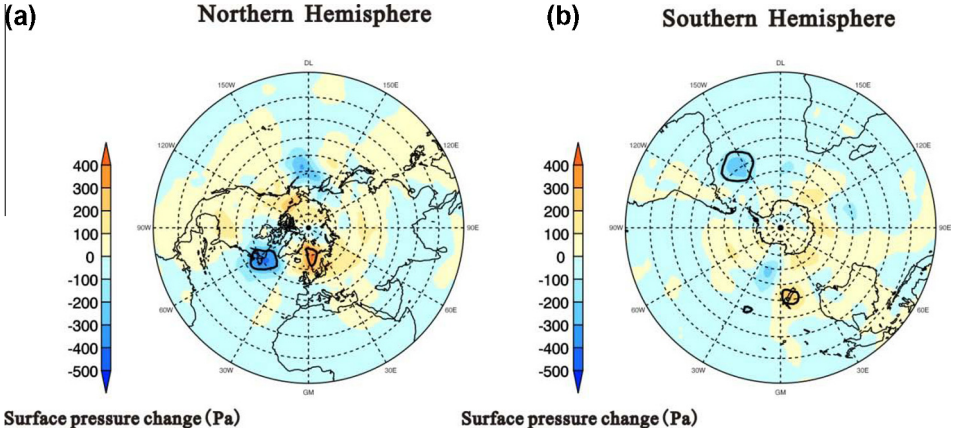

Fig. 6. The difference of the surface pressure of day 0 from that of day −3 with days defined such that day 0 is the day of minimum in the solar wind speed in winter with high volcanic activity. Key days are as in Figs. 2–4 (November–March 1963–2011). The solid dark lines are the boundary of the region where the statistical confidence is over 99% with the *t*-test.

summer in the southern hemisphere, so these regions centered south of the equator and increasing altitude are those of maximum exposure to solar UV.

In Fig. 9, a significant negative correlation (over 99% confidence) between solar wind geo-effective electric field and geopotential height can be seen at the 1000 hPa level, which is in a similar location to that of the solar flux correlation in Fig. 8. There is now a significant positive correlation in the Sahara region. These correlations weaken with increasing tropospheric altitude, but in the stratosphere the positive correlation again appears, even stronger than for 10.7 cm solar flux, and again increasing with altitude in the stratosphere where there is maximum exposure to solar UV.

Fig. 10 shows the spatial distribution of the correlation between SWS and geopotential height at five levels (a)–(e) of pressure in the northern summer. There is no clear and significant result at any level.

Fig. 11 shows in annual means the spatial distribution of the correlation between geopotential height at three pressure levels, 1000 hPa, 100 hPa and 10 hPa, for SWS, (a)–(c); solar wind electric field (d)–(f); and 10.7 cm solar

Please cite this article in press as: Zhou, L., et al. Effects on winter circulation of short and long term solar wind changes. J. Adv. Space Res. (2013), http://dx.doi.org/10.1016/j.asr.2013.09.017

Table 1
The correlation coefficients between solar activity parameters and the extratropical circulation indices, NAO and AO.

	NAO	AO	SWS	Sunspot	10.7 cm solar flux	SWS*Bz
*(a) Correlation coefficients for all the northern hemisphere winters (DJF) of the years 1963–2011 (48 winters) *with 95% confidence, **with 99% confidence*						
NAO	1	0.895**	0.454**	0.160	0.231	0.183
AO		1	0.332*	0.150	0.223	0.191
SWS			1	−0.081	−0.093	0.250
sunspot				1	0.977**	0.716**
10.7 cm solar flux					1	0.658**
*(b) Correlation coefficients for DJF in high volcanic activity eras, 1963–1966, 1983–1985 and 1992–1995 (9 winters) *with 95% confidence, ** with 99% confidence*						
NAO	1	0.878**	0.676*	0.329	0.686*	0.691*
AO		1	0.489	0.461	0.536	0.719*
SWS			1	0.355	0.536	0.766*
sunspot				1	0.747*	0.669*
10.7cm solar flux					1	0.658
*(c) Correlation coefficients for DJF in low volcanic activity eras (39 winters) *with 95% confidence, ** with 99% confidence*						
NAO	1	0.905**	0.385*	0.156	0.206	0.100
AO		1	0.300	0.133	0.199	0.126
SWS			1	−0.131	−0.140	−0.119
sunspot				1	0.975**	0.735**
10.7 cm solar flux					1	0.685**

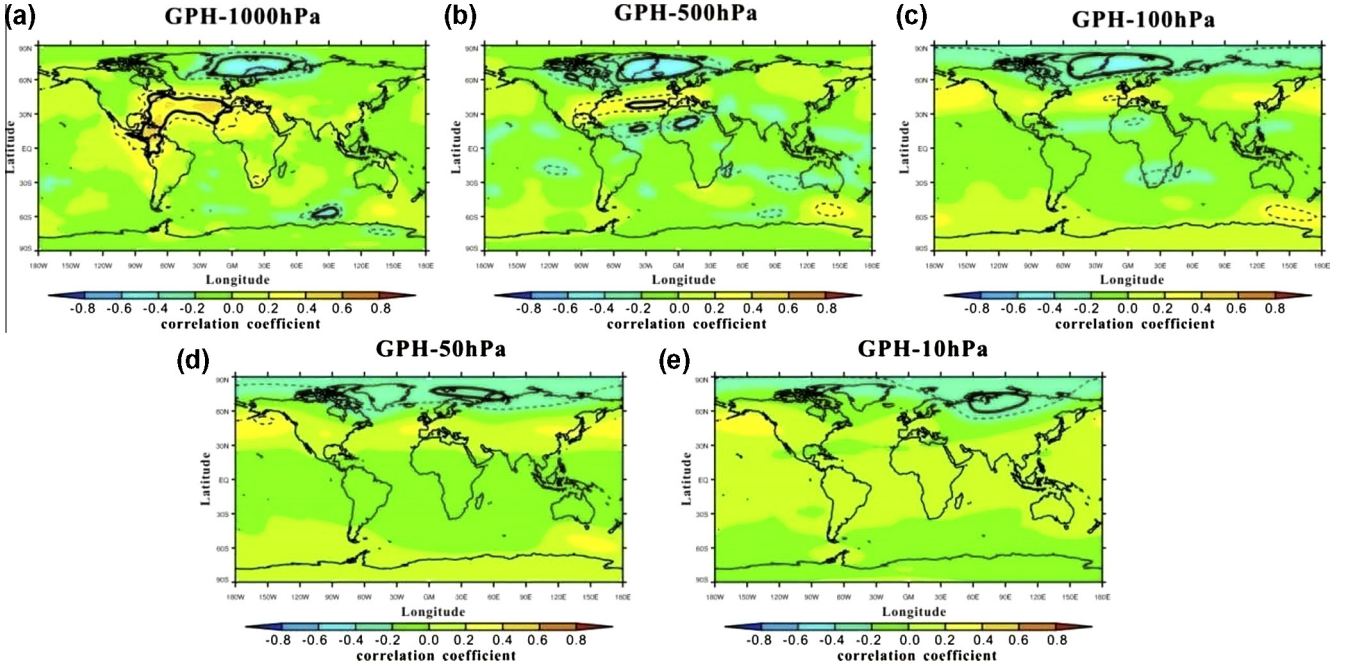

Fig. 7. The spatial distribution of the correlation between the SWS and geopotential height changes at five levels of pressure (1000 hPa, 500 hPa, 100 hPa, 50 hPa and 10 hPa) for winters (DJF average) from 1963 to 2011. The solid dark lines are the boundary of the region where the statistical confidence is over 99% and the dashed dark lines are the boundary of the region where the statistical confidence is over 95%.

flux for (g)–(i). On the annual time scale and for correlations with SWS, the only significant positive correlation is for the geopotential height at the 1000 hPa level in the North Atlantic Ocean region and no significant correlation signal can be found in the stratosphere. These annual mean correlations with E and the 10.7 cm solar flux both have high correlations in the stratosphere as in Figs. 8 and 9, with stronger correlations extending down to 1000 hPa than in the northern winters of Figs 7 and 8. However these annual patterns do not resemble the NAO pattern as much as that for the SWS. For the 10.7 cm solar flux, the stratospheric correlations are not as high as for the geo-effective electric field at any level.

4. Discussion

4.1. The possible linkage mechanism between SWS and the lower atmosphere

On the day to day time scale, for northern hemisphere winters, and as noted in the introduction, a significant response of atmospheric dynamics to the solar wind

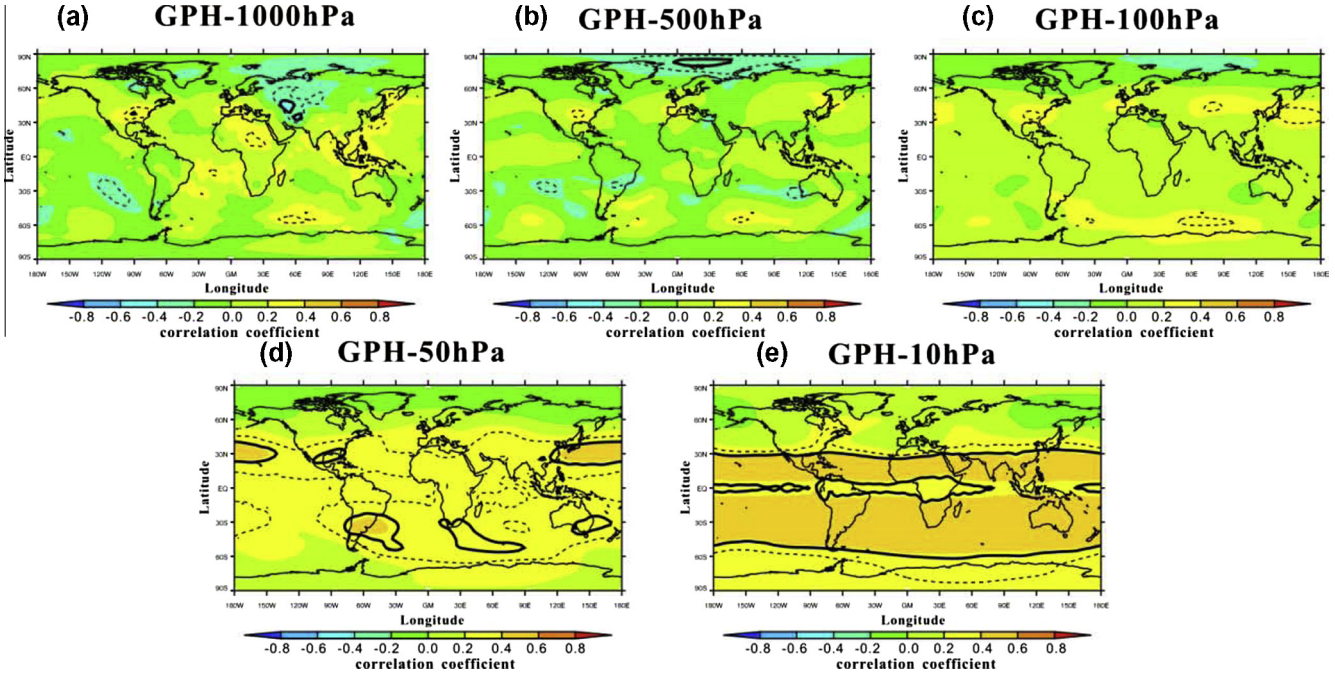

Fig. 8. As for Fig. 7, but for spatial correlation between the 10.7 cm solar flux and geopotential height changes.

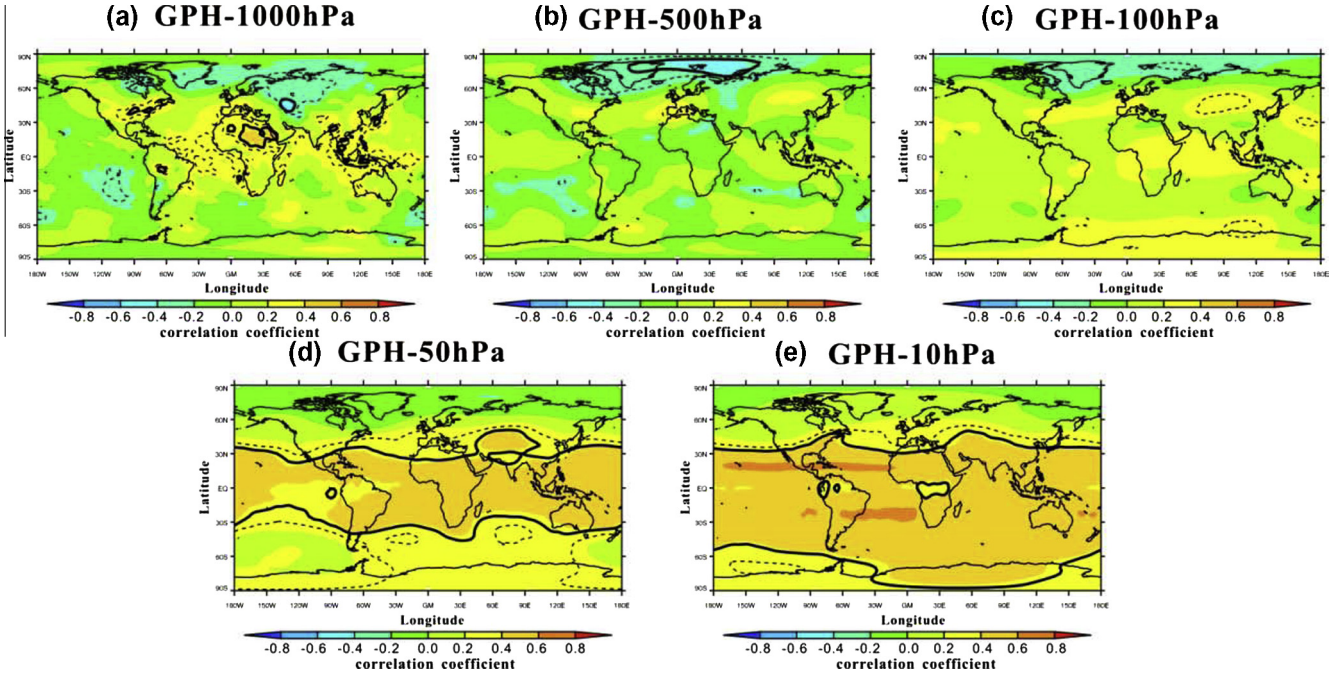

Fig. 9. As for Fig. 7, but for spatial correlation between the geo-effective solar wind electric field and geopotential height changes.

parameters has been shown in observations during the last half century by the superposed epoch analysis (Roberts and Olson 1973; Wilcox et al., 1973; Svalgaard, 1973; Kirkland et al., 1996; Mironova et al., 2012; Tinsley et al., 2012). These, and the day-to-day responses of the tropospheric regional dynamics shown in Figs 2, 3 and 6, have a time scale too small to be due to wave – mean flow interactions between the stratosphere and troposphere. Such interactions were described by Baldwin and Dunkerton (2001) and suggested by Boberg and Lundstedt (2002) as an explanation for their observations of regional dynamic response to the solar wind on the winter to winter timescale.

An explanation for the present and previous results that has a short enough timescale is that of electrical coupling from the solar wind, through the effects of its fields and particles (including REF and cosmic rays) on the global

Please cite this article in press as: Zhou, L., et al. Effects on winter circulation of short and long term solar wind changes. J. Adv. Space Res. (2013), http://dx.doi.org/10.1016/j.asr.2013.09.017

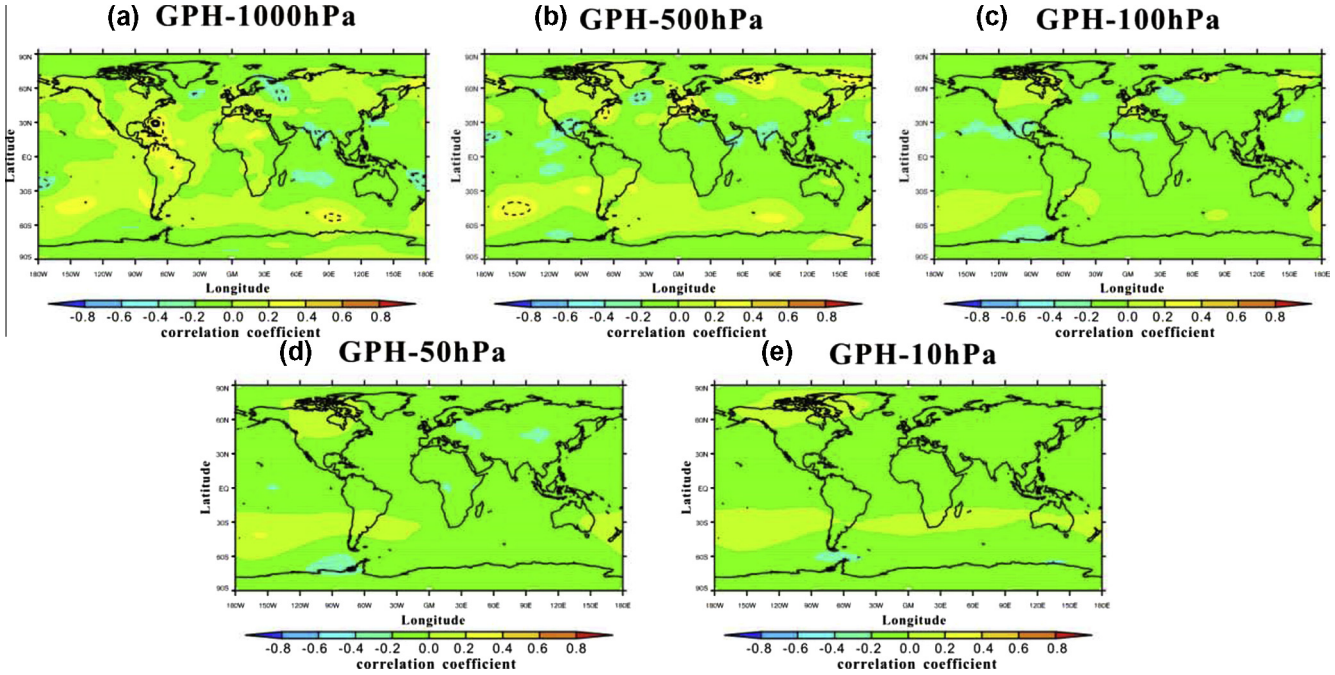

Fig. 10. As for Fig. 7, but for spatial correlation in northern hemisphere summer, June–July–August (1963–2011), between the SWS and geopotential height changes.

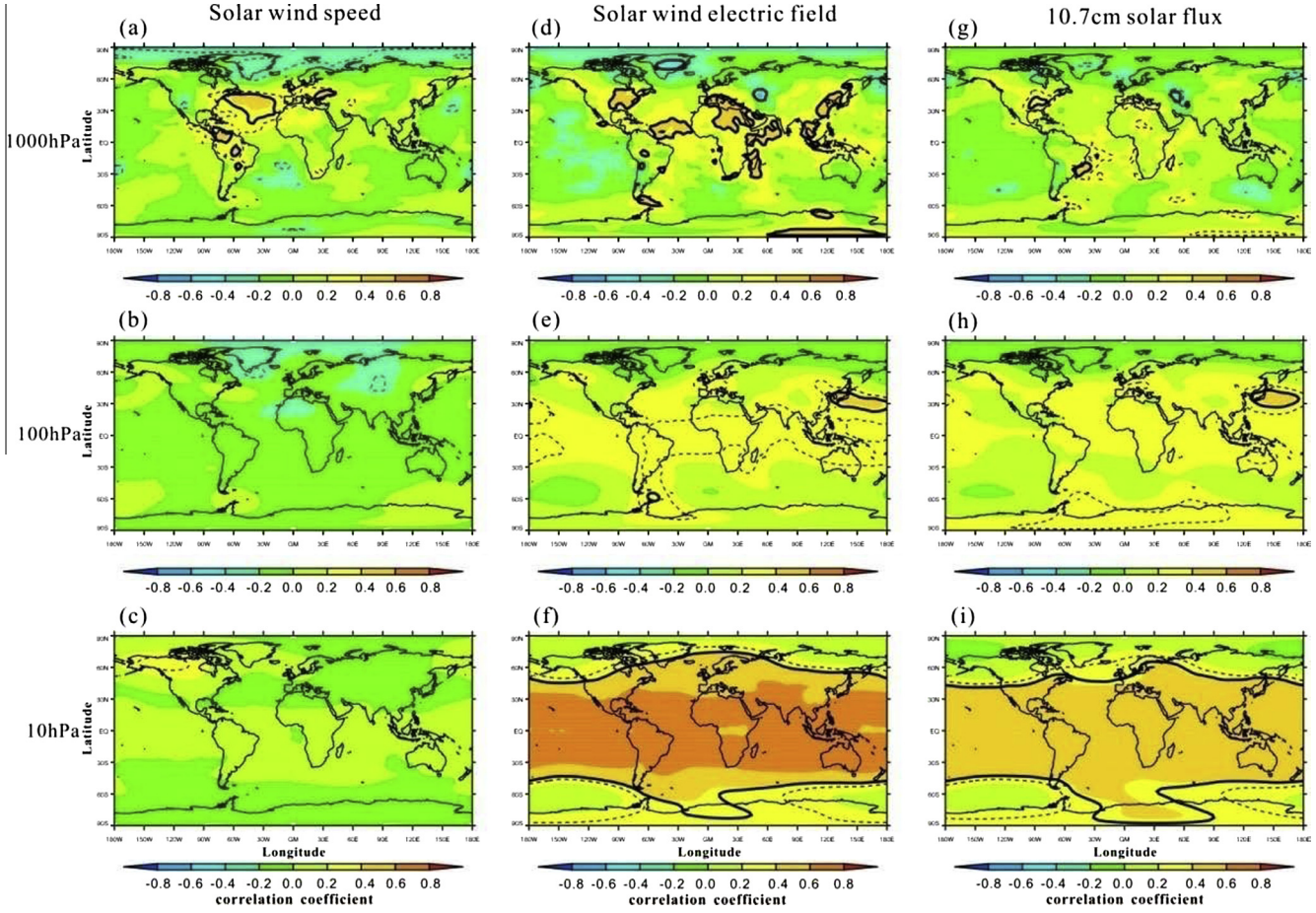

Fig. 11. Annual mean spatial correlations for geopotential height at three pressure levels (1000 hPa, 100 hPa, and 10 hPa) with the solar wind speed (a)–(c); solar wind geo-effective electric field (d)–(f); and 10.7 cm solar flux (g)–(i). The solid dark lines are the boundaries of the regions where the statistical confidence is over 99% and the dashed dark lines are the boundary of the region where the statistical confidence is over 95%.

Please cite this article in press as: Zhou, L., et al. Effects on winter circulation of short and long term solar wind changes. J. Adv. Space Res. (2013), http://dx.doi.org/10.1016/j.asr.2013.09.017

electric circuit, and it has a timescale of response of order of a day or less (Tinsley, 2008). It has been shown by Kirkland et al. (1996) and Tinsley et al. (2012) that the atmospheric dynamical response to REF depends on the presence of volcanic aerosol in the stratosphere, following the conversion of SO_2 and H_2O from eruptions into H_2SO_4 aerosol. It has been shown (as in Fig. 5) that the SWS determines the flux of relativistic electrons precipitating from the radiation belts at subauroral latitudes, and that these ionize the air in the stratosphere. When there is a high loading of volcanic aerosol, the modulation of the resulting higher stratospheric column resistance by the relativistic electron precipitation modulates the current flowing from the ionosphere down to the surface at subauroral latitudes. This has been simulated for an aerosol layer arbitrarily located at 40 km by Tinsley and Zhou (2006). Thus the electric current density flowing into clouds will be sensitive to the solar wind speed changes, and affect the distribution of electric charge (unipolar or space charge) in the clouds (Zhou and Tinsley, 2007, 2012; Nicoll and Harrison, 2011).

These charges can affect scavenging of nuclei in the clouds by changing the rates of collision with droplets of ice-forming nuclei and condensation nuclei (Tinsley and Leddon 2013). The greatest fluxes of precipitating relativistic (MeV) electrons are found in the sub-auroral zone, and so on the day-to-day timescale the surface pressure response is expected where there are extensive clouds present, as in the north Atlantic region in winter. The data of Fig. 6 showing lower pressure in the Labrador-Newfoundland area and higher pressure in the Scandinavia area contributes to a more negative NAO phase, consistent with the VAI responses discussed in the Introduction, and a weakening of cyclogenesis.

Mechanisms responsible for the tropospheric responses must be able to amplify by many orders of magnitude the energy input from the global electric circuit. There are two immediately apparent amplification mechanisms which can affect atmospheric dynamics. One is described by Tinsley (2012) in which the electrically enhanced scavenging of cloud condensation nuclei alters their size distribution and results in less initial precipitation from cumulonimbus clouds, with greater transport of water above the freezing level. This gives energy amplification by the enhanced release of latent heat of freezing.

Another amplification mechanism is that changes in cloud cover, e.g., in layer clouds, can result from electrically-induced scavenging of condensation and ice-forming nuclei. The cloud cover changes ensure energy amplification by changes in the long wave and shortwave radiative balance between the surface and cloud layer. Observations reported by Kniveton and Tinsley (2004) showed changes in zonal mean cloud cover related to the same changes in REF during high stratospheric aerosol years as in the present work.

Within the two classes of mechanisms there are a number of scavenging pathways, as discussed by Tinsley and Leddon (2013). Since both classes of amplification mechanisms affect, and are affected by, atmospheric dynamics, feedback on each other and within each may be important. While such cloud links are speculative, they are consistent with the evidence for a chain of rapid links from the SWS to pressure distributions in the lower atmosphere. Clarifying the details of the mechanisms and pathways and feedbacks involved will require much further research.

Besides the SWS, other space parameters such as solar radiation including ultraviolet (represented by sun spot number or 10.7 cm solar flux), and galactic cosmic ray flux also might affect surface pressure by other mechanisms. However, in Fig. 4 there is no significant change of 10.7 cm solar flux, sunspot number and GCR flux with the minima of solar wind speed. So it can be concluded that the day to day changes in Figs. 2, 3 and 6 are mainly controlled by SWS and Bz, and that other space weather parameters have little impact on these timescales.

4.2. SWS effect on climate

Although on the day to day time scale strong evidence for a physical link between solar wind speed and lower atmosphere pressure has been given, it is not necessarily the case that this by itself can significantly impact longer term climate. Also, on timescales longer than a few weeks, the effects of other space weather parameters and solar UV may also be present, and it could be hard to distinguish the effect of one input from another. The stratospheric responses that are shown in Figs 8, 9 and 11 have such a different character from the tropospheric responses that we suggest that they are independently generated. They are present all-year and extend further into the summer hemisphere than into the winter hemisphere. A combination of mechanisms relating to UV inputs and particle precipitation affecting stratospheric photochemistry seems to be the most plausible for these results. It is of interest that the presence of H_2SO_4 vapor and aerosols in the stratosphere, as well as NOx produced by the REP, would be likely to affect the photochemistry. Whether these stratospheric responses propagate to the surface in winter on a time scale of weeks, as suggested by Boberg and Lundstedt (2002), in addition to the day-to-day response that we have postulated to be electrical, remains to be determined. However, an increase in both the direct electrical and the downward propagation of stratospheric responses would be consistent with the increase in correlation coefficients of the NAO and AO with the SWS, the SWS*Bz, and the 10.7 cm flux in Table 1b, compared to those in Table 1c and a.

Of course, on climate timescales, the minima in SWS and SWS*Bz are not in themselves important, nor are the accompanying minima in the relativistic electron precipitation into the stratosphere at sub-auroral latitudes. These minima should be considered only as diagnostics for REP geo-effectiveness. What is important for climate are variations in the almost continuous flux of REP, and even more

Please cite this article in press as: Zhou, L., et al. Effects on winter circulation of short and long term solar wind changes. J. Adv. Space Res. (2013), http://dx.doi.org/10.1016/j.asr.2013.09.017

importantly, in the continuous flow of current density through clouds. The current density is affected not only by the relativistic electron flux and other external inputs such as galactic cosmic rays and solar wind electric fields, but by internal atmospheric inputs such as changes in thunderstorm output and volcanic activity.

5. Conclusions

Day to day superposed epoch analysis of the SWS and the extratropical circulation indexes, NAO and AO shows that there is a significant physical linkage between them, which is not consistent with downward propagation of changes from stratospheric levels. Winter average spatial correlation analysis implies that this link may also be effective when whole winters are compared. The possible physical mechanism could be a link via the global electric circuit and electrical enhancement of in-cloud scavenging processes. The SWS and its geo-effective components appear to be important parameters for research into sun climate linkages.

Acknowledgements

This work has been funded in part by Grant 2012CB957804 of the National Key Research Science Programmes of China; by NSFC Grant (41271054); and the US National Science Foundation Grant AGS 0836171.

References

Baldwin, M.P., Dunkerton, T.J., 2001. Stratospheric harbingers of anomalous weather regimes. Science 294, 581–584.

Boberg, F., Lundstedt, H., 2002. Solar wind variations related to fluctuations of the North Atlantic Oscillation. Geophys. Res. Lett. 29 (15), 1718. http://dx.doi.org/10.1029/2002GL014903.

Boberg, F., Lundstedt, H., 2003. Solar wind electric field modulation of the NAO: a correlation analysis in the lower atmosphere. Geophys. Res. Lett. 30 (15), 1825. http://dx.doi.org/10.1029/2003GL017360.

Burns, G.B., Tinsley, B.A., French, W.J.R., Troshichev, O.A., Frank-Kamenetsky, A.V., 2008. Atmospheric circuit influences on ground-level pressure in the Antarctic and Arctic. J. Geophys. Res. 113, D15112. http://dx.doi.org/10.1029/2007JD009618.

Eddy, J.A., 1976. The Maunder minimum. Science 192, 1189–1202.

Fleitmann, D., Burns, S.J., Mudelsee, M., Neff, U., Kramers, J., Mangini, A., Matter, A., 2003. Holocene forcing of the Indian monsoon recorded in a stalagmite from Southern Oman. Science 300, 1737–1739.

Fischer, H.J., Mühleisen, R., 1980. The ionospheric potential and the solar magnetic sector boundary crossings. Rep. Astron. Inst. Univ. Tübingen, Ravensburg, Germany 10, D-7980.

Goodman, J., Snetsinger, K.G., Pueschel, R.F., Ferry, G.V., 1994. Evolution of Pinatubo aerosol near 19 km altitude over western North America. Geophys. Res. Lett. 21 (12), 1129–1132.

Gray, L.J., Beer, J., Geller, M., Haigh, J.D., et al., 2010. Solar influences on climate. Rev. Geophys. 48, RG4001. http://dx.doi.org/10.1029/2009RG000282.

Kirkland, M.W., Tinsley, B.A., Hoeksema, J.T., 1996. Are stratospheric aerosols the missing link between tropospheric vorticity and Earth transits of the heliospheric current sheet? J. Geophys. Res. 101, 29689–29699.

Kniveton, D.R., Tinsley, B.A., 2004. Daily changes in global cloud cover and Earth transits of the heliospheric current sheet. J. Geophys. Res. 109, D11201.

Li, X., Temerin, M., Baker, D.N., Reeves, G.D., Larsen, D., 2001a. Quantitative prediction of radiation belt electrons at geostationary orbit based on solar wind measurements. Geophys. Res. Lett. 28, 1887–1890.

Li, X., Baker, D.N., Kanekal, S.G., Looper, M., Temerin, M., 2001b. Long term measurements of radiation belts by SAMPEX and their variations. Geophys. Res. Lett. 28, 3827–3830.

Marsh, N., Svensmark, H., 2003. Galactic cosmic ray and El Nino Southern Oscillation trends in International Satellite Cloud Climatology Project D2 low-cloud properties. J. Geophys. Res. 108 (D6), 4195. http://dx.doi.org/10.1029/2001JD001264.

Mironova, I., Tinsley, B.A., Zhou, L., 2012. The links between atmospheric vorticity, radiation belt electrons, and the solar wind. Adv. Space Res. 50, 783–790. http://dx.doi.org/10.1016/j.asr.2011.03.043.

Nicoll, K., Harrison, G., 2011. Charge measurements in stratiform cloud from a balloon based sensor. J. Phys. Conf. Ser. (301), 012003. http://dx.doi.org/10.1088/1742-6596/301/1/012003, ISSN: 1742–6588.

Reichler, T., Kim, J., Manzini, E., Kröger, J., 2012. A stratospheric connection to Atlantic climate variability. Nat. Geosci. 5, 783–787. http://dx.doi.org/10.1038/ngeo1586.

Reiter, R., 1977. The electric potential of the ionosphere as controlled by the solar magnetic sector structure. Result of a study over the period of a solar cycle. J. Atmos. Terr. Phys. 39, 95–99.

Roberts, W.O., Olson, R.H., 1973. Geomagnetic storms and wintertime 300-mb trough development in the North Pacific – North America area. J. Atmos. Sci. 30, 135–140.

Reeves, G.D., Morley, S.K., Friedel R.H.W., et al., 2011. On the relationship between relativistic electron flux and solar wind velocity: Paulikas and Blake revisited. J. Geophys. Res. 116. A02213 and auxiliary material.

Svalgaard, L., 1973. Solar activity and the weather. In: Page, D.E. (Ed.), 'Correlated Interplanetary and Magnetospheric Observations' Astrophysics and Space Science Library. Reidel, Dordrecht, Holland, pp. 627–639.

Thompson, D.W.J., Wallace, J.M., 1998. The Arctic Oscillation signature in the wintertime geopotential height and temperature fields. Geophys. Res. Lett. 25, 1297–1300.

Tinsley, B.A., 2005. On the variability of the stratospheric column resistance in the global electric circuit. Atmos. Res. 76, 78–94.

Tinsley, B.A., 2008. The global atmospheric electric circuit and its effects on cloud microphysics. Rep. Prog. Phys. 71, 066801. http://dx.doi.org/10.1088/1034-4885/71/6/066801.

Tinsley, B.A., 2012. A working hypothesis for connections between electrically-induced changes in cloud microphysics and storm vorticity, with possible effects on circulation. Adv. Space Res. 50, 791–805.

Tinsley, B.A., Deen, G., 1991. Apparent tropospheric response to MeV – GeV particle flux variations: a connection via electrofreezing of supercooled water in high-level clouds? J. Geophys. Res. 96, 22283–22296.

Tinsley, B.A., Leddon, D.B., 2013. Charge modulation of scavenging in clouds: extension of Monte Carlo simulations and initial parameterization. J. Geophys. Res. 118, 8612–8624. http://dx.doi.org/10.1002/jgrd.50618.

Tinsley, B.A., Zhou, L., 2006. Initial results of a global circuit model with stratospheric and tropospheric aerosols. J. Geophys. Res. 111, D16205.

Tinsley, B.A., Hoeksema, J.T., Baker, D.N., 1994. Stratospheric volcanic aerosols and changes in air–earth current density at solar wind magnetic sector boundaries as conditions for the Wilcox tropospheric vorticity effect. J. Geophys. Res. 99, 16805–16813.

Tinsley, B.A., Zhou, L., Liu, W., 2012. The role of volcanic aerosols and relativistic electrons in modulating winter storm vorticity. Adv. Space Res. 50, 819–827.

Please cite this article in press as: Zhou, L., et al. Effects on winter circulation of short and long term solar wind changes. J. Adv. Space Res. (2013), http://dx.doi.org/10.1016/j.asr.2013.09.017

Veretenenko, S., Thejll, P., 2004. Effects of energetic solar proton events on the cyclone development in the North Atlantic. J. Atmos. Solar-Terr. Phys. 66, 393–405.

Visbeck, M.H., Hurrell, J.W., Polvani, L., Cullen, H.M., 2001. The North Atlantic Oscillation: past, present, and future. Proc. Natl. Acad. Sci. USA 98, 12876–12877.

Wang, Y.J., Chen, H., et al., 2005. The holocene Asian monsoon: links to solar charges and North Atlantic climate. Science 308, 854–857.

Wilcox, J.M., Scheerer, P.H., Svalgaard, L., Roberts, W.O., Olson, R.H., 1973. Solar magnetic structure, relation to circulation in the Earth's atmosphere. Science 180, 185–186.

Zhou, L., Tinsley, B.A., 2007. The production of space charge in clouds. J. Geophys. Res. 112, D11203. http://dx.doi.org/10.1029/2006JD007998.

Zhou, L., Tinsley, B.A., 2012. Time dependent charging of layer clouds in the global electric circuit. Adv. Space Res. 50, 828–842. http://dx.doi.org/10.1016/j.asr.2011.12.18.

Please cite this article in press as: Zhou, L., et al. Effects on winter circulation of short and long term solar wind changes. J. Adv. Space Res. (2013), http://dx.doi.org/10.1016/j.asr.2013.09.017